Development 128, 1831-1843 (2001)
Printed in Great Britain © The Company of Biologists Limited 2001
DEV3394

Genetic dissection of *nodal* function in patterning the mouse embryo

Linda A. Lowe, Satoru Yamada* and Michael R. Kuehn‡

Experimental Immunology Branch, Division of Basic Sciences, National Cancer Institute, National Institutes of Health, Bethesda, MD 20892, USA

*Present address: Department of Periodontology and Endodontology, Osaka University Faculty of Dentistry, 1-8 Yamadaoka, Suita, Osaka 565-0871, Japan

‡Author for correspondence (e-mail: mkuehn@mail.nih.gov)

Accepted 23 February; published on WWW 19 April 2001

SUMMARY

Loss-of-function analysis has shown that the transforming growth factor-like signaling molecule nodal is essential for mouse mesoderm development. However, definitive proof of nodal function in other developmental processes in the mouse embryo has been lacking because the null mutation blocks gastrulation. We describe the generation and analysis of a hypomorphic *nodal* allele. Mouse embryos heterozygous for the hypomorphic allele and a null allele undergo gastrulation but then display abnormalities that fall into three distinct mutant phenotypic classes, which may result from expression levels falling below critical thresholds in one or more domains of *nodal* expression. Our analysis of each of these classes provides conclusive evidence for *nodal*-mediated regulation of several developmental processes in the mouse embryo, beyond its role in mesoderm formation. We find that nodal signaling is required for correct positioning of the anteroposterior axis, normal anterior and midline patterning, and the left-right asymmetric development of the heart, vasculature, lungs and stomach.

Key words: *nodal*, Anteroposterior axis, Left-right asymmetry, Node, Lateral plate mesoderm, Mouse

INTRODUCTION

Gastrulation in the vertebrate embryo results in the formation of the three germ layers and the establishment of the primary body axes, the anteroposterior (AP), dorsoventral (DV) and left-right (LR) axes. In the mouse, gastrulation initiates with the formation of mesoderm at the primitive streak, a transient structure at the posterior of the embryo. Mutational studies have revealed an essential role for nodal, a transforming growth factor β-related signaling molecule, in the early steps of mouse gastrulation (Conlon et al., 1991; Conlon et al., 1994; Iannaccone et al., 1992; Zhou et al., 1993). Embryos homozygous for the retroviral insertional mutation that originally identified the *nodal* gene fail to form a primitive streak and lack morphological evidence of embryonic mesoderm (Conlon et al., 1994; Iannaccone et al., 1992; Pfendler et al., 2000). The early expression pattern of *nodal* in the normal mouse embryo is consistent with a role in gastrulation. Expression is found prior to gastrulation in the proximal epiblast, then becomes restricted to the posterior embryonic ectoderm as the streak forms and elongates (Varlet et al., 1997). *nodal*-related genes have been identified in other vertebrates, including chick, *Xenopus* and zebrafish (Feldman et al., 1998; Jones et al., 1995; Levin et al., 1995; Rebagliati et al., 1998b; Sampath et al., 1998; Smith et al., 1995). Zebrafish embryos with combined mutations in two *nodal*-related genes, *cyclops* and *squint*, also fail to form mesoderm (Feldman et al., 1998). Ectopic expression studies in *Xenopus* and zebrafish embryos have shown that nodal and related factors can induce the formation of mesoderm (Jones et al., 1995; Joseph and Melton, 1997; Toyama et al., 1995). Additionally, approaches to specifically inhibit nodal signaling in frog embryos lead to a block in mesoderm formation (Agius et al., 2000; Osada and Wright, 1999). Taken together these studies provide strong evidence for a role for the nodal signaling pathway in vertebrate mesoderm induction at the start of gastrulation.

In addition to a role in gastrulation, nodal has been implicated in LR development, in part owing to asymmetric domains of expression found at later stages. In head-fold and early somite stage mouse embryos, *nodal* is expressed in mesendodermal cells around the node (Conlon et al., 1994; Zhou et al., 1993). This transient embryonic structure and its derivatives, the notochord and prechordal plate, are key organizing centers for embryonic pattern formation. During early somite stages *nodal* expression around the node becomes progressively asymmetric, with stronger expression on the left side (Collignon et al., 1996; Lowe et al., 1996). At the same stages, *nodal* is also expressed in the lateral plate mesoderm (LPM) but only on the left side. Asymmetric expression is evolutionarily conserved, being found in every vertebrate examined (Collignon et al., 1996; Fujinaga et al., 2000; Levin et al., 1995; Lowe et al., 1996; Lustig et al., 1996; Rebagliati et al., 1998a; Sampath et al., 1998). It has been proposed that *nodal*, and other asymmetrically expressed genes since identified, act in a molecular pathway directing normal LR asymmetric development of the heart, and other visceral organs (reviewed in Burdine and Schier, 2000; Capdevila et al., 2000). Although misexpression of nodal on the right side of chick and

Xenopus embryos is sufficient to alter organ asymmetry (Levin et al., 1997; Sampath et al., 1997), a requirement for nodal signaling in mouse LR development has not been unequivocally shown, owing to the early arrest of the nodal null mutant. Indirect evidence for such a role has come from genetic studies. In mouse and zebrafish mutants with LR defects, asymmetric expression of *nodal* or the zebrafish *nodal*-related *cyclops* is perturbed (Collignon et al., 1996; Heymer et al., 1997; Izraeli et al., 1999; Lowe et al., 1996; Melloy et al., 1998; Rebagliati et al., 1998a; Sampath et al., 1998). Mutations in mouse *cryptic* or zebrafish *one eyed pinhead* cause LR defects (Yan et al., 1999). These genes encode related EGF/CFC extracellular proteins that are required for nodal signaling (Gritsman et al., 1999; Kumar et al., 2001; Saijoh et al., 2000). Mouse embryos with a mutation in Smad2, which functions to transduce nodal signals (Kumar et al., 2001), show LR abnormalities when rescued beyond early gastrulation (Heyer et al., 1999). Embryos heterozygous for both a *nodal* null mutation and mutation in Smad2 also show LR defects (Nomura and Li, 1998). However, chimeras with a high percentage of Smad2 mutant cells undergo normal LR development (Tremblay et al., 2000), complicating the interpretation of the compound heterozygotes. In addition, certain mutant alleles of *cyclops*, presumed to be nulls, do not alter LR patterning of the zebrafish heart (Chen et al., 1997). Furthermore, no LR defects were reported in mouse chimeras made with a large contribution of *nodal* mutant cells (Varlet et al., 1997). Therefore it is still an open question whether nodal is necessary for patterning the LR axis.

Nodal signaling also has been implicated in anterior neural development. Anterior defects were found in mouse chimeras made with normal and *nodal* mutant cells, in which the visceral endoderm was composed exclusively of *nodal* mutant cells (Varlet et al., 1997). Mouse embryos heterozygous for mutations in both *nodal* and Smad2 also show anterior defects including cyclopia (Nomura and Li, 1998). Zebrafish mutations in either of the *nodal*-related genes, *cyclops* or *squint*, result in anterior patterning defects (Feldman et al., 1998; Hatta et al., 1991; Heisenberg and Nusslein-Volhard, 1997). However, the *cyclops* and *squint* mutations both cause midline defects that may interfere with proper anterior patterning, suggesting that nodal may be involved only indirectly in anterior patterning.

A loss-of-function analysis of *nodal* in LR and anterior development is impossible with the original *nodal* mutant, owing to its early developmental arrest. Therefore, we have used a Cre/loxP strategy (reviewed by Marth, 1996) to make a conditional mutant allele flanked by loxP site-specific recombination signals (floxed). This floxed allele can undergo Cre-mediated deletion, leading to loss of function. Homozygotes are viable and fertile, and so can be used in conjunction with stage- and tissue-specific Cre transgenic lines to carry out conditional mutational analysis of nodal function. In the course of characterizing the floxed allele, we discovered that although floxed homozygotes were normal, embryos that were compound heterozygotes for the floxed and a *nodal* null allele were not. These results were found in the absence of any Cre-mediated recombination, indicating that the floxed allele is hypomorphic. Embryos with reduced nodal function undergo gastrulation but then display abnormalities, which fall into distinct phenotypic classes, at later stages. We have carried out a comprehensive analysis of these phenotypes and provide conclusive evidence for nodal regulation of multiple developmental processes in the mouse embryo, beyond its role in mesoderm formation.

MATERIALS AND METHODS

Gene targeting

The *nodal* cDNA was used to isolate an 18 kilobase (kb) genomic clone from a 129Sv lambda library. An 8 kb *Bam*HI fragment covering the upstream region, the first exon, the first intron and 165 basepairs of the second exon, and the 3′ contiguous 4.5 kb *Bam*HI fragment covering the rest of the gene and 2 kb downstream were subcloned. These fragments were modified by PCR to introduce a loxP site into the first intron and another loxP site after the 3′ untranslated region. They were then combined with a fragment of the *nodal* cDNA that contained the remainder of the second exon and the third exon up to the stop codon, as well as a fragment that contained the IRES beta geo cassette (Mountford et al., 1994). Details of the construction are available upon request. The final arrangement is shown in Fig. 1A. The loxP sites were tested by transformation of 294-Cre bacteria (Buchholz et al., 1996). For gene targeting the vector was linearized and transfected by electroporation into W9.5 embryonic stem (ES) cells (Buzin et al., 1994). ES cell culture and blastocyst injections were carried out by standard methods.

Mouse breeding and genotyping

Male germline chimeras were bred with C57Bl6/J females to obtain F_1 animals carrying the floxed *nodal* allele (*nodal*^{fl1}), and with 129/Sv females for inbreeding. To derive animals carrying a deleted *nodal* allele (*nodal*$^{\Delta}$), we bred *nodal*^{fl1} animals with EIIa-Cre mice. Embryos derived from EIIa-Cre transgenic females express Cre in all cells of the early embryo (Lakso et al., 1996). Offspring from this cross with the deleted allele were identified by Southern blotting of *Eco*RI digests (probe shown in Fig. 1A). Subsequent genotyping was by PCR. The following PCR genotyping primers were used: for the wild-type allele, F114/NI2 CCCAGCAAATGCAAACTGACC (specific for *nodal* intron 2) and R403/n3U ACGTTTCTGCTCCCTGGAT-AGAC (specific for the 3′UTR of *nodal*) for the floxed allele, F580/neo CCGAATATCATGGTGGAAAATGGC (specific for the neo gene) and R403/n3U; for the *nodal*$^{\Delta}$ allele, R878 AGTTCCCCACACCTCACATAACC (specific for *nodal* intron 2); and F654 AGAACCAGAAGAGGGATTTGGG (specific for the 3′UTR of *nodal*).

Phenotypic and molecular analysis

Analysis of cardiac and vasculature malformations was by colored latex injections into right and left ventricles (Oh and Li, 1997). Whole-mount in situ hybridization was carried out as described (Lowe and Kuehn, 2000). Whole-mount X-gal staining to check *lacZ* expression was performed by a modification of existing protocols. Briefly, embryos were fixed in 0.2% Glutaraldehyde, 5 mM EDTA, 2 mM $MgCl_2$, 1× PBS at room temperature for 30 minutes to 1 hour, then immediately placed in 5 mM $K_4Fe(CN)_6$, 5 mM $K_3Fe(CN)_6$, 1× PBS, 2 mM $MgCl_2$, 2 mg/ml X-gal in DMSO and kept at room temperature overnight. Selected embryos were embedded in JB-4 plastic and sectioned as described (Lowe and Kuehn, 2000).

RESULTS

Generating a floxed allele of *nodal*

We used a promoterless targeting vector to introduce loxP sites around the *nodal*-coding region by homologous recombination in ES cells (Fig. 1A). An IRES-βgeo cassette (Mountford et al., 1994) was placed immediately after the *nodal* stop codon.

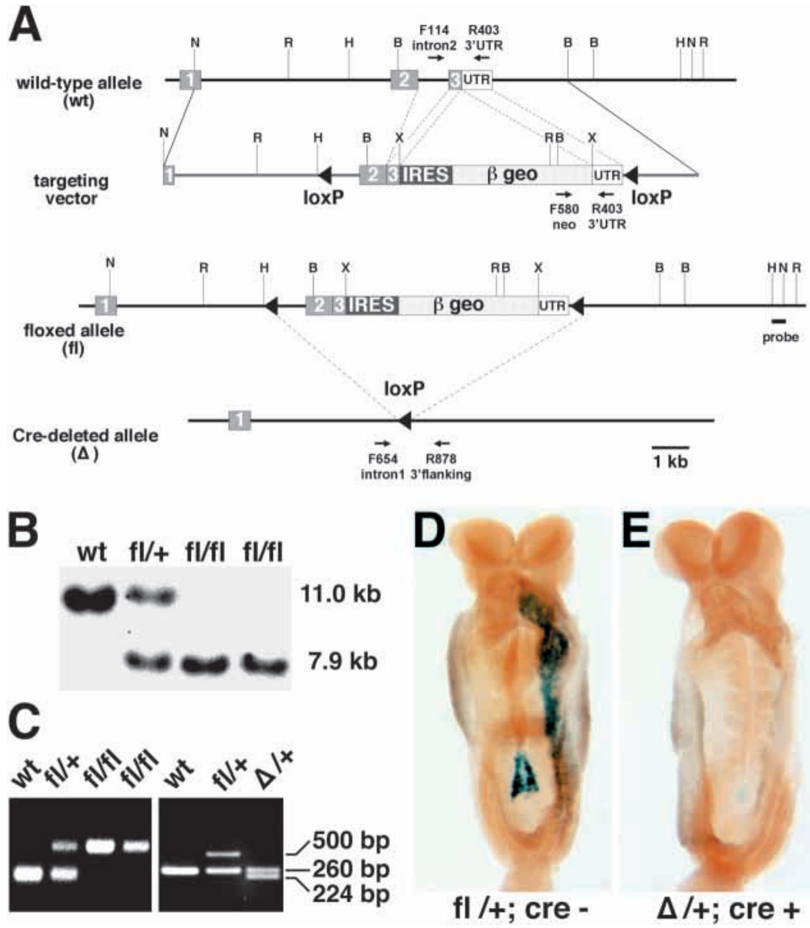

Fig. 1. Generating a floxed *nodal* (*nodal*^{fl1}) allele. (A) Map of targeting vector and *nodal*^{fl1}allele resulting from homologous recombination. Location of PCR primers and probe used for Southern analysis are shown. N, *Not*I; R, *Eco*RI; H, *Hin*dIII; B, *Bam*HI; X, *Xba*I. (B) Southern analysis of *Eco*RI-digested DNA from wild type (wt), and from *nodal*^{fl1} heterozygotes (fl/+) and homozygotes (fl/fl). The probe shown in A detects an 11.0 kb wt fragment and a 7.9 kb *nodal*^{fl1} fragment. (C) Left: PCR analysis of tail DNA, confirming *nodal*$^{fl1/fl1}$ genotype. Right: PCR analysis of embryo DNA from crosses of heterozygous *nodal*^{fl1} and EIIa-Cre animals using all five genotyping primers. (D,E) X-gal-stained E8.5 embryos, viewed ventrally with anterior towards the top. D shows a *nodal*^{fl1} heterozygote with staining in the node and left LPM reproducing the nodal mRNA expression pattern. The embryo in E carries the EIIa-Cre transgene, and shows loss of staining indicating deletion of the *nodal*^{fl1} allele.

This results in a bicistronic message encoding *nodal* as well as providing G418 selection of transfectants and expression of β-galactosidase (β-gal) with a pattern identical to *nodal*. One loxP site was placed within the first intron and another immediately 3′ to the IRES-βgeo cassette. We assumed that loss of this part of the coding sequence, following Cre-mediated recombination, would eliminate function because it encodes the secreted, mature region of nodal. The 3′ loxP site was positioned after the IRES-βgeo to allow the extent of Cre-mediated recombination to be assessed in situ, by monitoring colorimetrically the loss of β-gal activity.

We expected to enrich for homologous recombinants using the promoterless targeting strategy. Remarkably, in two separate experiments, greater than 95% of G418-resistant colonies were homologous recombinants. Two pools of five to six homologously recombined ES cell clones were used to establish two lines of *nodal*^{fl1} mice. Breeding of *nodal*^{fl1} heterozygotes on a mixed genetic background (129/Sv and C57Bl/6J) produced the expected number of homozygotes (Fig. 1B,C). Further breeding showed that homozygotes were viable and fertile. Whole-mount X-gal staining of embryonic day (E) 6.5, E7.5 and E8.5 embryos gave a pattern that was essentially the same as that of wild-type *nodal* mRNA expression (Lowe et al., 1996; Fig. 1D). To confirm that the *nodal*^{fl1} allele is capable of undergoing Cre-mediated recombination, we crossed *nodal*^{fl1} males with EIIa-Cre females (Lakso et al., 1996). As expected for this Cre transgenic strain, in which all cells of the early embryo express Cre, PCR analysis of offspring revealed the specific product resulting from deletion between the loxP sites (Fig. 1C). In addition, embryos collected from these matings revealed almost complete loss of X-gal staining (Fig. 1E), indicating that the *nodal*^{fl1} allele can be efficiently recombined by Cre to produce the deleted allele (*nodal*$^{\Delta}$).

The *nodal*^{fl1} allele is a hypomorph

Analysis of embryos with a *nodal*$^{\Delta/\Delta}$ genotype showed a pre-gastrulation block identical to the original *nodal* insertional mutant, confirming that the *nodal*$^{\Delta}$ allele is a null. Unexpectedly, *nodal*$^{fl1/\Delta}$ embryos were found that had undergone gastrulation but were clearly abnormal. These embryos did not carry Cre. This result indicated that a single copy of the floxed allele is insufficient for normal development. Analysis of additional embryos (n=133) obtained from crossing *nodal*$^{+/\Delta}$ mice with *nodal*^{fl1} homozygotes, none carrying Cre, revealed 41% with overt developmental defects at E7.5. A sample set was genotyped and all phenotypically abnormal embryos were *nodal*$^{fl1/\Delta}$. Of the abnormal embryos, 6% were arrested at the pre-gastrulation stage and the remaining 35% had clearly undergone gastrulation. Of the embryos examined at E8.5 (n=542), 46% were abnormal with 6% arrested prior to gastrulation and the remainder showing post-gastrulation defects. Although a small percentage of *nodal*$^{fl1/\Delta}$ embryos appeared normal at these early stages, those found alive at E14.5 were abnormal and PCR genotyping of four litters (n=21) showed that no *nodal*$^{fl1/\Delta}$ pups survived to birth. These findings confirm that the floxed *nodal* allele has reduced function, i.e. is hypomorphic. As described in the sections below, detailed analysis of the defects caused by the hypomorphic allele has provided new insight into nodal function not revealed by the *nodal* null mutant, identifying several developmental processes for which nodal signaling is crucial.

Positioning of the AP axis is abnormal in *nodal* hypomorphic mutants

Examination of E7.5 *nodal*$^{fl1/\Delta}$ embryos showed morphological abnormalities as well as alterations in the pattern of *nodal* expression, as detected by X-gal staining for

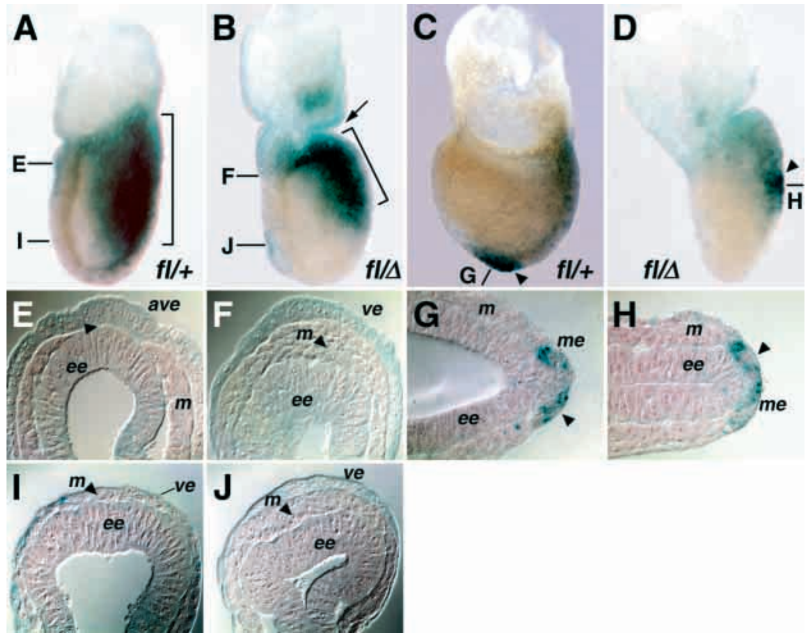

Fig. 2. Abnormalities in E7.5 *nodal*$^{fl1/\Delta}$ embryos. (A-D) Embryos X-gal stained for β-gal activity, viewed laterally with anterior towards the left. (E-J) Transverse sections from the embryos directly above them, taken at the positions indicated. (E,F,I,J) Anterior is towards the top. (G) Distal is to the right. (H) Posterior is towards the right. (A) A *nodal*$^{fl1/+}$ (fl/+) embryo with a pattern of staining indicating normal nodal expression in the primitive streak (bracketed). (B) A similarly staged *nodal*$^{fl1/\Delta}$ (fl/Δ) embryo. Staining (bracketed) does not extend as far distally and there is a constriction at the embryonic/extra-embryonic boundary (arrow). (C) An older *nodal*$^{fl1/+}$ embryo showing staining in the node (arrowhead). (D) A similarly staged *nodal*$^{fl1/\Delta}$ embryo showing abnormally positioned staining (arrowhead) and a constriction. (E) Proximal cross section of the embryo in A revealing the normal direct contact (arrowhead) between the anterior visceral endoderm (ave) and the embryonic ectoderm (ee). Mesoderm, m. (F) Section of the embryo in B revealing the abnormal accumulation of mesoderm (arrowhead) between the embryonic ectoderm and visceral endoderm (ve). (G) Section of the embryo in C. Staining is apparent in the mesendodermal cells (me) around the node (arrowhead). (H) Section of the embryo in D. Staining is also seen in mesendodermal cells (arrowhead). (I) Distal cross section of the embryo in A showing the normal accumulation of mesoderm (arrowhead) between the thin squamous visceral endoderm layer and the embryonic ectoderm. (J) Distal cross section of the embryo in B showing the thick layer of mesoderm (arrowhead) between the embryonic ectoderm and the abnormally cuboidal visceral endoderm.

β-gal expressed from the *nodal*^{fl1} allele. Normally at the primitive streak/early head-fold stage, *nodal* is expressed in the posterior embryonic ectoderm, extending the length of the primitive streak (Fig. 2A). Expression in *nodal*$^{fl1/\Delta}$ embryos did not extend as far distally from the embryonic/extra-embryonic boundary (Fig. 2B), suggesting truncation of the primitive streak. We also found a constriction at the boundary between the embryonic and extra-embryonic regions in mutants (Fig. 2B). In normal embryos, the anterior visceral endoderm (AVE) is a morphologically distinct group of cells at the anterior midline close to the embryonic/extra-embryonic boundary (Fig. 2E). In *nodal*$^{fl1/\Delta}$ embryos, the morphology of the visceral endoderm at the embryonic/extra-embryonic boundary was different from that in a normal AVE (Fig. 2F). Normally, there is direct contact between the AVE and the underlying anterior embryonic ectoderm (Fig. 2E). In *nodal*$^{fl1/\Delta}$ embryos, the lateral edges of the mesodermal wings encroached on the anterior midline at this position (Fig. 2F). Interestingly, visceral endoderm cells with a distinct cuboidal shape were found in a distal location (Fig. 2J), where visceral endoderm is normally squamous (Fig. 2I). This might represent an abnormally located AVE, but there was also mesoderm between these cells and the embryonic ectoderm (Fig. 2J). In the normal embryo, primitive streak expression ceases by the neural plate stage. *nodal* is then expressed in mesendodermal cells of the node forming at the anterior end of the primitive streak, which is at the distal tip of the embryo (Fig. 2C,G). In mutants at this stage, localized expression was found only half way down the posterior side (Fig. 2D). This position coincided with the distal-most limit of primitive streak expression found in embryos examined at earlier stages (Fig. 2B). These *nodal*-expressing cells appeared to be mesodermal or mesendodermal as in a normal node (Fig. 2H), suggesting node development in a more proximal location. It has been proposed that the AP axis arises from a 90° rotation of the pre-existing proximal-distal axis of the pregastrulation embryo (Beddington and Robertson, 1998; Beddington and Robertson, 1999). The altered position of primitive streak and node expression, together with the apparently misplaced AVE, suggests that axial rotation does not occur properly in *nodal*$^{fl1/\Delta}$ embryos.

To analyze AP axis rotation further, we examined *brachyury*, *Hesx1/Rpx* and *Otx2* expression. Each of these genes is expressed asymmetrically along the nascent AP axis (Hermesz et al., 1996; Herrmann, 1991; Simeone et al., 1993). *brachyury* is found first in pre-streak stage normal embryos in the proximal embryonic ectoderm (Thomas et al., 1998). Expression then shifts posteriorly, marking in succession the primitive streak (Fig. 3A), node and notochord (Fig. 3C,E,G). In contrast to *nodal*-null mutants, which express *brachyury* only transiently or not at all (Conlon et al., 1994; Pfendler et al., 2000), *nodal* hypomorphs do show primitive streak *brachyury* expression. However, the domain was foreshortened and located more proximally than in normal embryos (Fig. 3B,D,H). Some *nodal* hypomorphs had a distinct node showing *brachyury* expression. However, the node was found in a more proximal location than normal (Fig. 3C,D,E,F). Further anteriorly, *brachyury* expression was reduced and discontinuous in the midline in some *nodal*$^{fl1/\Delta}$ embryos (Fig. 3G,H,I,J). In normal embryos, *Otx2* is expressed throughout the embryonic ectoderm and visceral endoderm before and during early gastrulation, and then becomes restricted to the anterior ectoderm and visceral endoderm (Fig. 3K,M). In *nodal*$^{fl1/\Delta}$ mutants, *Otx2* expression was consistently found more distally than normal (Fig. 3L,N). *Hesx1/Rpx* normally is expressed anteriorly, both in the AVE and in the overlying

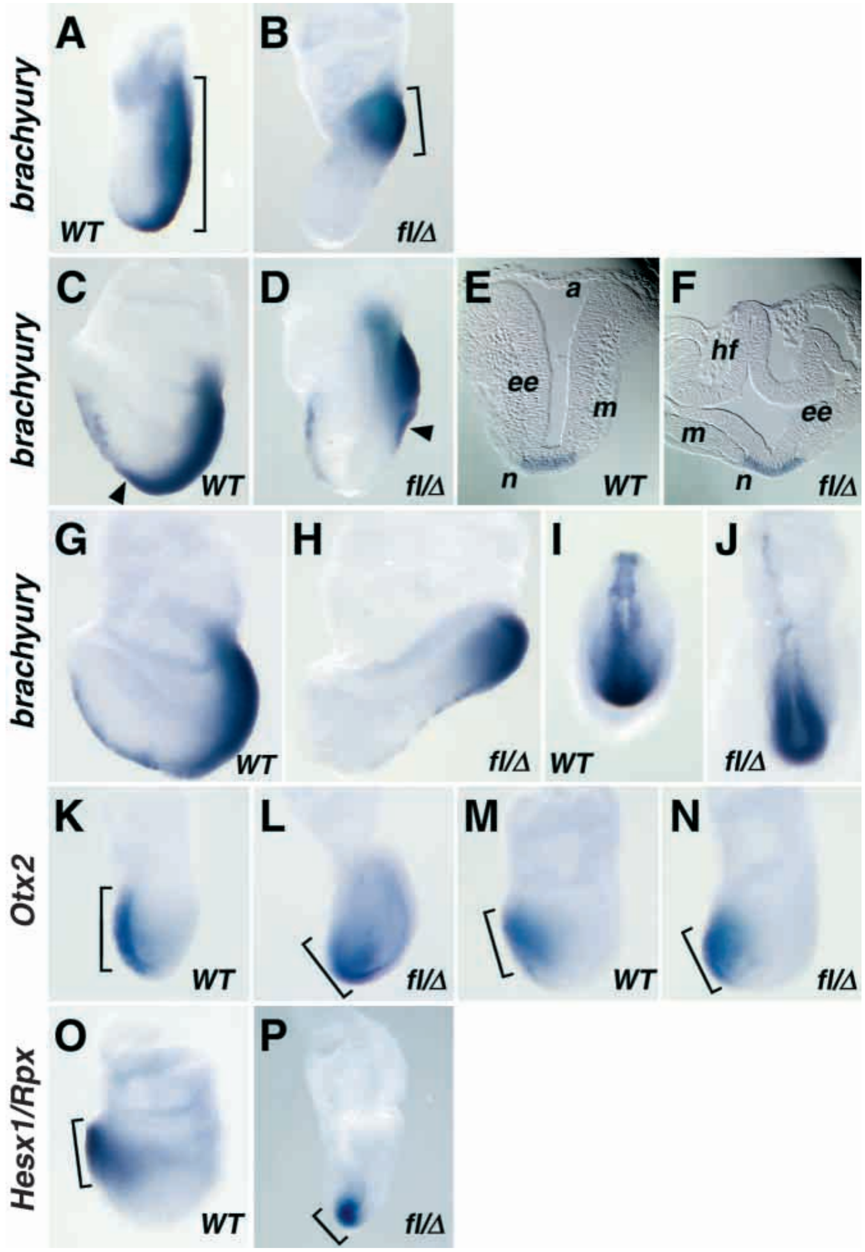

Fig. 3. Analysis of markers of AP positioning at E7.5. All embryos are shown laterally with anterior toward the left, except in I and J where embryos are viewed ventrally with anterior toward the top. (E,F) Transverse sections through the node of the embryos in C,D, respectively, at the positions indicated by the arrowheads. (A) Wild type (WT) mid-primitive streak embryo with *brachyury* expression throughout the streak (bracketed). (B) Mid-primitive streak *nodal*$^{fl1/\Delta}$ (fl/Δ) embryo with proximal *brachyury* expression (bracketed). (C) Mid-head-fold stage WT embryo expressing *brachyury* in the primitive streak, node (arrowhead) and anterior axial mesendoderm. (D) Mid-head-fold stage *nodal*$^{fl1/\Delta}$ embryo with truncated primitive streak *brachyury* expression and a more proximally located node (arrowhead). (E) Cross section of the embryo in C showing *Brachyury* expression in the ventral node (n). At this angle of sectioning, the node lies in a plane with the amnion (a). Embryonic ectoderm, ee; mesoderm, m. (F) Cross section of the embryo in D, showing *brachyury* expression in the ventral node. Owing to altered AP positioning, the node lies in a plane with the head folds (hf). (G) Late head-fold stage WT embryo, with primitive streak, node and notochord *brachyury* expression. (H) Late head-fold stage *nodal*$^{fl1/\Delta}$ embryo with truncated primitive streak *brachyury* expression. (I) Ventral view of the embryo in G. (J) Ventral view of the embryo in H, showing reduced midline *brachyury* expression. (K) WT mid-primitive streak embryo with anterior *Otx2* expression (bracketed). (L) Mid-primitive streak *nodal*$^{fl1/\Delta}$ embryo showing distal *Otx2* expression (bracketed). (M) Early head-fold stage WT embryo showing anterior *Otx2* expression (bracketed). (N) Early head-fold stage *nodal*$^{fl1/\Delta}$ embryo with more distal *Otx2* expression (bracketed). (O) Early head-fold stage WT embryo with anterior *Hesx1/Rpx* expression (bracketed). (P) A *nodal*$^{fl1/\Delta}$ embryo showing distal *Hesx1/Rpx* expression.

neural plate by the start of gastrulation (Fig. 3O). In *nodal* hypomorphs, *Hesx1/Rpx* expression also was located more distally than normal (Fig. 3P). Together these data indicate an early nodal function in the axial rotation that establishes the normal position of cells along the AP axis.

The AP axial positioning defects seen at E7.5 were more pronounced by E8.5. Analysis of mutant embryos (n=219) revealed three distinct phenotypic classes (Fig. 4A-C). One class, which represented 20% of mutants, developed with the anterior region outside the yolk sac (Fig. 4B). Another 29% of mutants developed completely outside the yolk sac (Fig. 4C). The remaining 51% developed normally within the yolk sac and constituted another class that we hereafter refer to as Type I. Embryos that developed partially and completely outside the yolk sac are designated as Type II and Type III mutants, respectively.

Defective anterior patterning in *nodal* hypomorphic mutants correlates with anterior midline mesendodermal defects

One feature shared by all three mutant classes was a severe defect in anterior patterning. Compared with normal embryos (Fig. 4A), Type II and Type III embryos had an abnormal ventral orientation of the head without any obvious demarcation into distinct fore-, mid- and hindbrain regions (Fig. 4B,C). Type I embryos consistently lacked the normal ventral midline separation of the anterior neural folds at E8.5 (Fig. 4D,E,H,I), and displayed holoprosencephaly at E14.5 (Fig. 4F,G). To examine patterning of the brain further in all three phenotypic classes we again analyzed *Otx2* expression. In normal E8.5 embryos, *Otx2* is restricted to the anterior neurectoderm where the fore- and mid-brain regions develop (Fig. 4H). This pattern was undisturbed in Type I mutants (Fig.

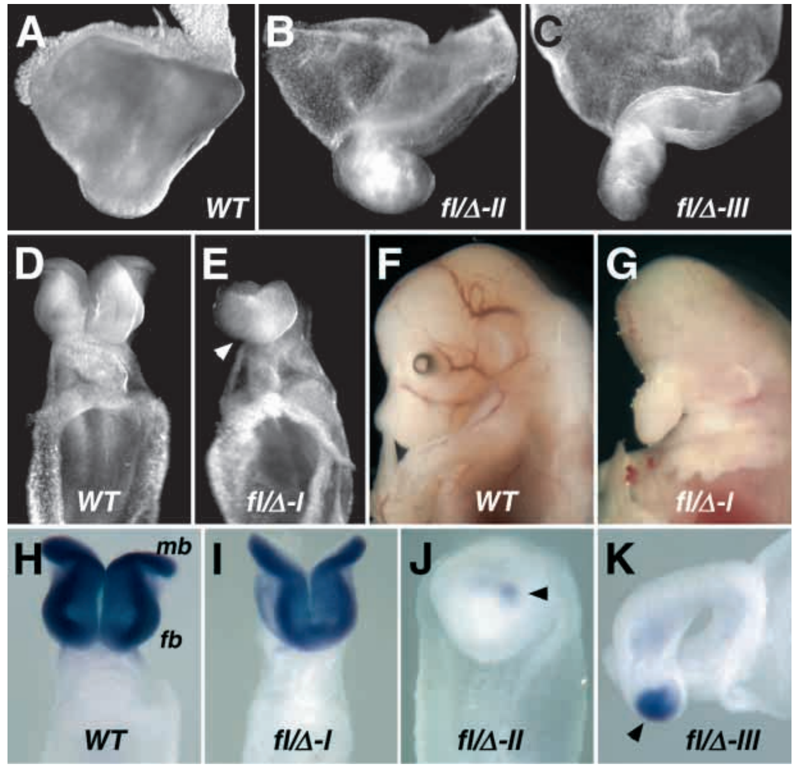

Fig. 4. Anterior patterning defects in *nodal*$^{fl1/\Delta}$ embryos. E8.5 embryos in A-C are viewed with anterior towards the left and ventral towards the bottom. E8.5 embryos in D,E,H-J are viewed ventrally. E14.5 embryos in F,G are viewed from the left side. (A) WT embryo enclosed in the extra-embryonic membranes. Type I *nodal*$^{fl1/\Delta}$ embryos showed the same arrangement. (B) Type II *nodal*$^{fl1/\Delta}$ embryo (fl/Δ-II) showing the anterior region developing outside the yolk sac. (C) Type III *nodal*$^{fl1/\Delta}$ embryo (fl/Δ-III) developing completely outside the yolk sac. (D) WT embryo with cranial neural folds showing a clear midline demarcation. (E) Type I *nodal*$^{fl1/\Delta}$ embryo (fl/Δ-I). The head is small and there is no midline separation in the forebrain (arrowhead). (F) WT embryo. (G) Type I embryo showing an abnormally shaped cranium and snout, and lacking eyes. (H) WT embryo showing *Otx2* expression in the midbrain (mb) and forebrain (fb). (I) Type I mutant embryo showing apparently normal *Otx2* expression. (J) Type II mutant embryo showing reduced *Otx2* expression in the head (arrowhead). (K) Lateral view of an E8.5 Type III mutant embryo with *Otx2* expression restricted to the extreme anterior (arrowhead).

4I). In contrast, in both Type II and Type III mutants *Otx2* expression was reduced and restricted to a small anterior domain (Fig. 4J,K).

In normal embryos, both the AVE and the midline mesendoderm are thought to participate in head patterning (Camus et al., 2000; Tam and Steiner, 1999). Thus, the observed anterior patterning defects could have their origin in early AVE defects, or in problems in the midline mesendoderm, or both. To assess the state of the midline mesendoderm we examined the expression of *sonic hedgehog* (*Shh*), which is normally found in the node, notochord, prechordal plate and gut endoderm (Fig. 5A,F,I). In Type I embryos, *Shh* expression in the brain did not extend as far anteriorly as in normal embryos (Fig. 5A,B). Cross section analysis revealed the absence of prechordal plate in the forebrain region of type I embryos, and showed that the foregut also does not extend as far anteriorly as in normal embryos (Fig. 5F,G). However, an apparently normal *Shh*-expressing notochord was evident in the hindbrain and in the trunk region of Type I embryos (Fig. 5B,G). Type II mutants were found either with *Shh* expression in the midline (Fig. 5C) or without (Fig. 5D). In those with *Shh* expression, notochord was found in the trunk, ending abruptly just at the level of the head (Fig. 5H,J). *Shh*-negative Type II embryos lacked notochord completely (Fig. 5K). Cross section analysis revealed the abnormal ventral orientation of the head in Type II embryos, as well as the disorganization and repeated folding of the head neurectoderm (Fig. 5H). Type II embryos lacked a recognizable prechordal plate and foregut pocket, as well as a distinct floorplate in the trunk region (Fig. 5J,K). Type III embryos had a closed neural tube with an underlying notochord that expressed *Shh* (Fig. 5E,L). Notochord, and *Shh* expression, ended well short of the most anterior region, and no recognizable prechordal plate was found. These results suggest that ventral midline defects contribute to the anterior patterning abnormalities found in all three classes of mutant embryos.

Type II and Type III embryos also showed other phenotypic abnormalities in the midline, as well as in the gut. Type II embryos had abnormally narrow and prematurely closed hindguts (Fig. 5C,D). In Type III embryos, the only *Shh* expression found was in notochord, suggesting that this mutant class lacks gut endoderm. Indeed there was no morphologically recognizable gut tube in any Type III embryo. All Type II embryos had fusion of somites across the midline (Fig. 5J,K), regardless of the presence or absence of notochord. This was clearly demonstrated by analyzing *paraxis* (Burgess et al., 1995) gene expression. In normal E8.5 embryos, *paraxis* is found in the paired somites and presomitic mesoderm (Fig. 5M). Type II embryos showed either single broad somites in the mid-trunk (Fig. 5N) or complicated patterns of splitting and crossing over (Fig. 5O). Most Type III embryos had paired somites as in normal embryos (Fig. 5P), although some were found with fused somites or with only disorganized paraxial mesoderm (not shown).

Altered nodal expression in E8.5 *nodal* hypomorphic mutants

The midline mesendoderm defects described above may result from alterations in the development of the node, perhaps due to reduced *nodal* expression. Therefore, we examined all three classes of E8.5 hypomorphs both for the structure of the node and for expression from the *nodal*^{fl1} allele by X-gal staining. Normally at this stage, *nodal* is expressed around the node and in the left LPM (Fig. 6A,B,G,K). Surprisingly, all three mutant classes completely lacked left LPM expression (Fig. 6C-F,H-J). For Type I embryos there was an apparently normal level of X-gal staining around the node, which also appeared to be normal in structure (Fig. 6K,L). With X-gal staining it was difficult to detect asymmetry of *nodal* expression around the node in either floxed heterozygotes or Type I mutants (Fig. 6A,C). Analysis of *nodal* mRNA confirmed normal asymmetry in floxed heterozygotes. However, mRNA levels were too low to assess asymmetry in Type I mutants (not shown). Therefore, β-gal activity exaggerates *nodal* mRNA levels, and does not reflect the lower level that exists in Type I embryos compared with floxed heterozygotes. For Type II embryos, X-gal staining around the node was clearly reduced, suggesting extremely low *nodal* mRNA levels. The structure of the node was abnormal as well (Fig. 6E,I,M). Normally, *nodal*-positive cells lie at the periphery of the node (Fig. 6K). In Type II embryos, *nodal*-positive cells were found across the midline. In addition, endodermal or mesendodermal cells were found extending ventrally into the hindgut (Fig. 6M). For Type III embryos there was no recognizable node, nor any apparent LPM (Fig. 6J). However, X-gal staining was consistently found in mesodermal or mesendodermal cells in a discrete area in the presumed posterior end that may represent an abnormal node (Fig. 6F,N). These results suggest a function for nodal signaling in the formation of the node.

LR development is defective in Type I *nodal* hypomorphic mutants

The lack of LPM expression in mutants allowed us to test the hypothesis that *nodal* expression in the left LPM is essential for the correct LR asymmetric orientation of the heart. We restricted this analysis to Type I embryos because only this class developed a heart tube. We first analyzed *lefty-2* and *Pitx2*, two other genes also expressed asymmetrically in the left LPM of E8.5 normal embryos, and thought to be regulated by nodal signaling and to play a role in LR patterning. All Type I mutants (n=13) examined lacked *lefty-2* expression (Fig. 7A,B). Analysis of Type I embryos (n=5) for *Pitx2* revealed no LPM expression, although head and body wall mesoderm showed normal, symmetric levels of expression (Fig. 7C,D). We also found no *lefty-1*, normally expressed at this stage on the left side of the floorplate (Fig. 7A,B). Thus Type I embryos completely lack asymmetric gene expression in the left LPM and midline. To determine whether this affected cardiac

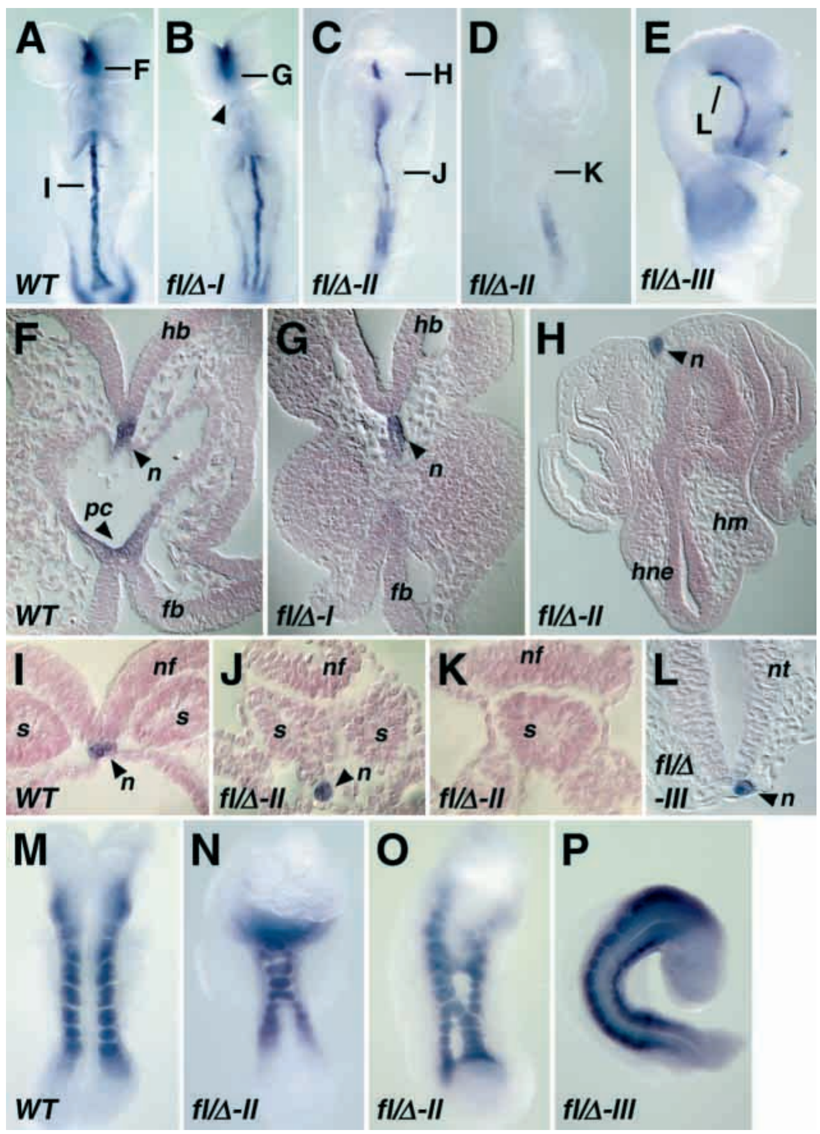

Fig. 5. Midline patterning defects in E8.5 $nodal^{fl1/\Delta}$ embryos. (A-E,M-P) Whole-mount in situ hybridization. (F-L) Transverse sections with dorsal toward the top. Embryos in A-D,N,O are viewed ventrally with anterior toward the top. (A) WT embryo showing normal *Shh* expression in the brain, midline and hindgut endoderm. (B) Type I embryo showing truncated *Shh* expression in the brain (arrowhead) but apparently normal trunk midline and hindgut expression. (C) Type II mutant with midline and hindgut *Shh* expression. (D) Type II mutant lacking midline *Shh* expression but with expression in the gut. (E) Type III embryo showing *Shh* expression along the AP axis. (F) Section through the brain of the WT embryo in A showing *Shh* expression in notochord of the hindbrain (hb) region and prechordal plate (pc) of the forebrain (fb) region. (G) Section through the brain of the Type I embryo in B. *Shh* is expressed in notochord in the hindbrain region but there is no prechordal plate. (H) Section through the head of the Type II embryo in C, which projects ventrally. *Shh* is expressed in the notochord. The head neurectoderm (hne) is extensively folded. hm, head mesenchyme. (I) Section through the WT embryo in A, showing *Shh* expression in the notochord of the trunk. nf, neural folds; s, somite. (J) Section through the Type II embryo in C, showing *Shh* expression in the trunk notochord. The neural folds are separated from the notochord by two midline somites. (K) Section through the Type II embryo in D showing the lack of trunk notochord, a single midline somite and flattened neural folds. (L) Section through the Type III mutant in E showing *Shh* expression in notochord adjacent to the neural tube (nt). (M) WT embryo viewed dorsally showing *paraxis* expression in the paired somites. (N) Type II embryo with *paraxis*-expressing somites fused across the midline and a ventrally displaced head. (O) Another Type II embryo showing somite fusions. (P) Type III embryo showing *paraxis* expression in paired somites.

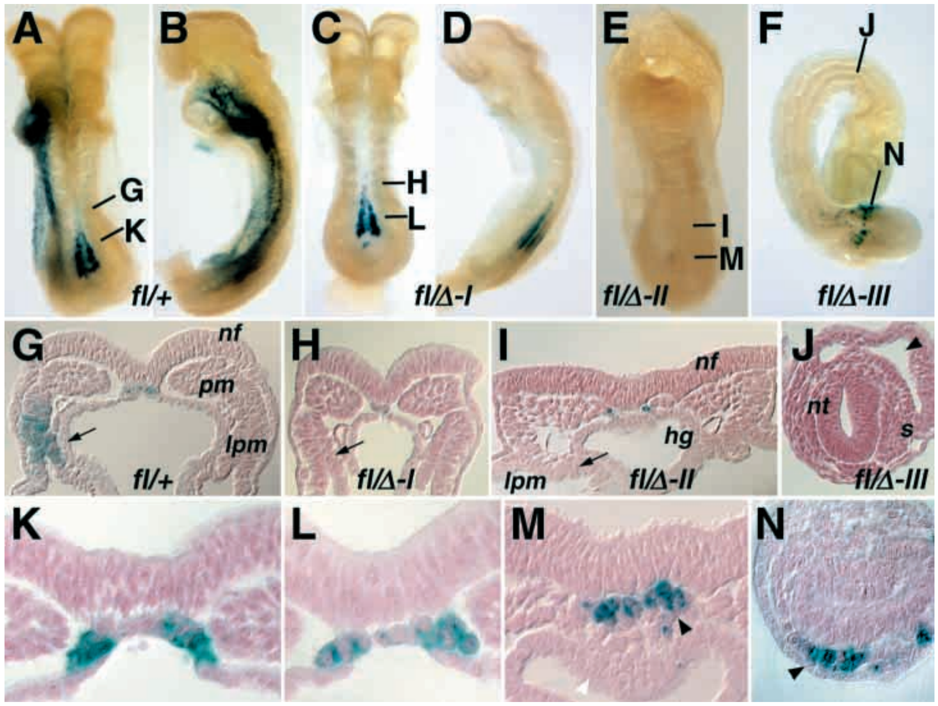

Fig. 6. Nodal expression in E8.5 *nodal*$^{fl1/\Delta}$ embryos. (A-F) Embryos X-gal stained for β-gal activity, viewed with anterior towards the top. (G-N) Transverse sections with dorsal towards the top. (A) A *nodal*$^{fl1/+}$ embryo viewed dorsally showing normal staining around the node and in the left LPM. (B) The same embryo viewed from the left side. (C) Type I *nodal*$^{fl1/\Delta}$ embryo viewed dorsally showing staining only in the node. (D) The same embryo viewed laterally, highlighting the lack of left LPM staining. (E) Type II embryo viewed dorsally, showing lack of staining in the LPM and reduced node staining. (F) Type III embryo showing expression at the presumed posterior. (G) Section of the embryo in A. X-gal staining is in the node and left LPM (arrow). nf, neural folds; pm, paraxial mesoderm. (H) Section of the Type I embryo in C. There is no staining in the LPM (arrow). (I) Section of the Type II embryo in E showing lack of staining in the LPM (arrow). The neural folds are flat and the hindgut (hg) is closed. (J) Section of the Type III embryo in F showing the lack of a recognizable LPM in the midtrunk region. There is a closed neural tube (nt), somite (s) and an unidentified body cavity (arrowhead). (K) Close-up of the node of the embryo in A. (L) Close-up of the node of the Type I embryo in C. (M) Close-up of the node region of the Type II embryo in E. Stained cells lie across the midline (black arrowhead) and cells have accumulated in the hindgut (white arrowhead). (N) Close-up of the posterior region of the Type III embryo in F showing X-gal stained mesodermal or mesendodermal cells (arrowhead).

development, we examined the direction of heart tube looping in E8.5 mutants. Although this process was delayed compared with normal littermates, approximately half of the mutant hearts that had undergone looping were reversed (Fig. 7E,F). This suggested that the loss of nodal expression from the left LPM causes randomization of heart asymmetry.

The continued viability of Type I embryos past E8.5 enabled us to examine later stages of heart development, as well as determine the importance of nodal signaling in the asymmetric patterning of other visceral organs. Examination of organ morphology in E13.5 to E14.5 Type I embryos (*n*=48) revealed multiple defects (Table 1). We found an equal incidence of hearts in which the apex was pointing rightward or leftward (Fig. 7G,H), and (regardless of orientation) the positions of the aorta and pulmonary trunk were always transposed. Normally the pulmonary trunk lies ventral to the aorta and connects to the right ventricle, whereas the aorta connects to the left ventricle. In latex marker experiments, yellow latex injected into the right ventricle of a normal heart was subsequently found in the pulmonary trunk, while injection of blue latex into the left ventricle labeled the aorta (Fig. 7I). However, in mutants yellow latex injected into the right ventricle was subsequently found in the aorta (Fig. 7J). In addition, sequential injection of yellow and blue latex into the right and left ventricles, respectively, resulted in mixing of the markers, indicating septation defects (Fig. 7J). Normally the right lung has four lobes and the left has one lobe (Fig. 7K). However, mutant lungs consistently showed four lobes on both the right and left sides (Fig. 7L). A fraction of the mutants had stomachs on the right side rather than the normal left-sided location (Fig. 7M,N). In others, rotation of the stomach was incomplete, leaving it close to the midline at the level of the lungs, but on either the left or right side (Fig. 7O,P). This analysis establishes that the nodal signaling pathway is required for proper asymmetric patterning of several visceral organs.

Table 1. Phenotypic analysis of LR defects in E14.5 *nodal*^{fl1}/*nodal*$^{\Delta}$ embryos

Organ or tissue	Phenotype	Frequency
Great vessels (*n*=48)	Normal	0
	Transposed	48 (100%)
Heart direction (*n*=48)	Normal	23 (48%)
	Reversed	25 (52%)
Lungs (*n*=48)	Normal, asymmetric	2 (4%)
	Abnormal, asymmetric	4 (8%)
	Right isomeric	42 (88%)
Stomach (*n*=45)	Normal left	37 (82%)
	Normal right	4 (9%)
	Midline left	1 (2%)
	Midline right	3 (7%)
Liver (*n*=46)	Normal appearance	30 (65%)
	Reduced size and/or pale	16 (35%)

DISCUSSION

The goal of this study was to generate a conditional allele to allow an analysis of post-gastrulation *nodal* function. Fortuitously, the floxed *nodal* allele we produced is also

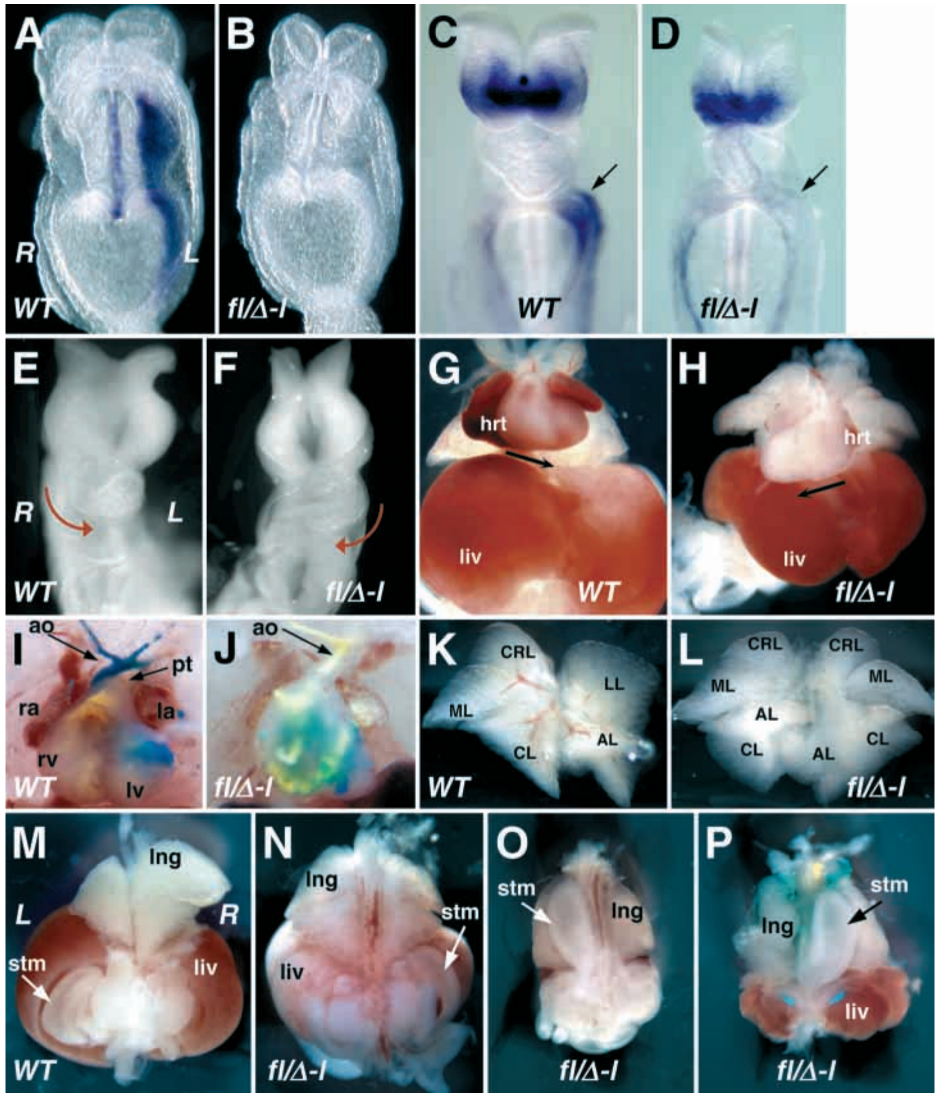

Fig. 7. LR patterning defects in Type I *nodal*$^{fl1/\Delta}$ mutants. (A-D) Whole-mount in situ hybridization. E8.5 embryos in A-F and viscera from E14.5 embryos in G-L are viewed ventrally. E14.5 viscera are viewed dorsally in M-P. (A) WT embryo with normal *lefty-2* expression in the left LPM and *lefty-1* expression in the left floorplate. R, right side; L, left side. (B) Type I embryo lacking expression of both *lefty* genes. (C) WT embryo with normal *Pitx2* expression in the left LPM (arrow) and head. (D) Type I embryo without *Pitx2* expression in the left LPM (arrow). (E) WT embryo showing normal rightward looping of the heart tube (red arrow). (F) Type I embryo showing reversed looping (red arrow). (G) WT visceral organs. The apex of the heart (hrt) points to the left (arrow). liver, liv. (H) Visceral organs of a Type I embryo. The apex of the heart points to the right (arrow). The liver is smaller than normal. (I) WT heart following sequential injection of yellow latex into the right ventricle (rv) and blue latex into the left ventricle (lv). Yellow latex has flowed into the pulmonary trunk (pt), connected to the right ventricle. Blue latex has flowed into the branching aorta (ao), connected more dorsally to the left ventricle. ra, right atrium; la, left atrium. (J) Type I heart after sequential latex injections. Yellow latex has flowed into the aorta, indicating an abnormal connection to the right ventricle. Extensive mixing of the blue and yellow latex in the heart indicates lack of septation. (K) WT lungs showing four right lobes, cranial (CRL), middle (ML), caudal (CL) and accessory (AL), and a single left lobe (LL). (L) Both left and right lungs of Type I embryos have four lobes. (M) WT visceral organs. The stomach (stm) is on the left, dorsal to the liver. (N) Visceral organs of a Type I embryo showing the stomach on the right. The liver is pale. (O) Visceral organs of a Type I embryo showing a left-sided stomach, which is undescended lying dorsal to the lungs. The liver and lungs are undersized. (P) Visceral organs of a Type I embryo with a right-sided undescended stomach. The liver and lungs are undersized.

hypomorphic, independent of Cre-mediated recombination. Expression of the floxed allele may be affected at the level of transcription or mRNA processing, owing to the presence of the IRES-βgeo cassette, which more than doubles the size of the transcript. The floxed allele combined with a *nodal*-null allele results in three distinct mutant phenotypic classes. These different classes may resulting from expression levels of the hypomorphic allele falling below critical thresholds in one or more of the multiple domains of *nodal* expression. Additionally, because nodal may regulate its own transcription and that of components of the nodal pathway (see below), reduced nodal levels at an early stage could have consequences for later domains of expression. Thus, each phenotypic class may reflect a unique conflation of specific temporal and spatial patterns of reduced nodal signaling. Our analysis of these classes provides direct evidence for nodal-mediated regulation of AP axial positioning, and anterior and midline patterning, and confirms a crucial role for this gene in mediating LR patterning of the viscera.

Nodal signaling is required for AP axial positioning and anterior patterning

It has been proposed that the proximal-distal axis of the pregastrulation embryo is transformed into the AP axis by cell movements that relocate visceral endoderm cells from the distal end of the embryo to the prospective anterior, and proximal embryonic ectoderm to the prospective posterior where the primitive streak then arises (Beddington and Robertson, 1998; Beddington and Robertson, 1999). Our analysis of *nodal* mutant embryos at E7.5 showed that expression of both *nodal* and *brachyury* was more proximally located that normal, closer to their position in pregastrulation embryos. Additionally, anterior markers were found to be in more distal locations than normal. These findings suggest that the proximal-distal to AP shift initiates in *nodal* hypomorphs but fails to complete. A more severe example of this phenotype, in which no movement occurs, is seen in mouse embryos with a targeted mutation in the EGF/CFC family member *cripto* (Ding et al., 1998). Importantly, members of the EGF/CFC family have been shown to be essential for nodal signaling (Gritsman et al., 1999; Kumar et al., 2001; Saijoh et al., 2000). Loss of function of another putative component of the nodal signaling pathway, the type IIA and IIB activin receptors, also leads to mislocalization of anterior and posterior markers, and a very similar overall phenotype to nodal hypomorphic mutants (Song et al., 1999). Finally, the phenotype of zebrafish that lack nodal function, either through mutations in *one-eyed pinhead* or in *cyclops* and *squint* combined, has been interpreted as showing AP positioning defects as well (Schier and Shen, 2000). Our results support a general requirement for early nodal signaling in assuring the proper movement of cells establishing the vertebrate AP axis.

The domain of nodal expression essential for mesoderm formation has been localized to the prestreak posterior embryonic ectoderm (Varlet et al., 1997). Only a small fraction of *nodal*$^{fl1/\Delta}$ embryos fail to gastrulate, indicating that in most mutants the level of nodal expression in this region is above the threshold required for mesoderm formation. Nodal signaling from the visceral endoderm has been implicated in proper anterior patterning (Varlet et al., 1997). This result has been a key part of a developing hypothesis that anterior patterning in the mouse embryo is regulated, at least in part, by a head organizer located in the AVE (Beddington and Robertson, 1998; Beddington and Robertson, 1999; Bouwmeester and Leyns, 1997). In contrast to the small number of *nodal*$^{fl1/\Delta}$ embryos that show a mesoderm formation defect, the majority shows anterior patterning defects, suggesting that nodal levels fall below a critical threshold in the visceral endoderm in most mutants. Although nodal signaling may function directly in neural induction, it is possible that reduced visceral endoderm signaling causes abnormal anterior patterning indirectly, through an effect on AP positioning. Normally the lateral wings of the more proximal mesoderm do not cross the midline. Thus, the AVE is in direct contact with the prospective anterior neurectoderm, which may be essential for any signaling function. In nodal hypomorphs, not only might the AVE be mispositioned, but there is also mesoderm separating the visceral endoderm from the embryonic ectoderm at every position along the anterior midline. This is presumably due to an altered direction of mesoderm migration originating in the abnormally positioned primitive streak. Encroachment of mesoderm across the anterior midline could have the consequence of interrupting all cell-cell signaling between the AVE and anterior ectoderm, including neural inducing signals. It is not necessary that nodal itself play a role in such signaling. In fact, *nodal* is not expressed uniquely in the AVE, but transiently and at a low level throughout the visceral endoderm. In addition, there is specific expression in the AVE of factors that may negatively regulate nodal function: *lefty-1* (Meno et al., 1999) and *cerberus-like* (*Cer1*) (Belo et al., 1997; Biben et al., 1998; Shawlot et al., 1998). Therefore it is possible that lowered nodal signaling in the visceral endoderm, although directly causing an incomplete proximal-distal to AP axial shift and thus improper positioning of cells along the AP axis, is only indirectly responsible for anterior patterning defects.

Nodal signaling is required for normal midline mesendoderm development

Our results indicate a required role for nodal signaling in the formation and function of the node and its derivatives including the notochord and prechordal plate, and the gut endoderm. The midline mesendoderm tissue plays a critical role in anterior development, perhaps by reinforcing and refining an initial unstable neural induction signal provided by the AVE (Bachiller et al., 2000; Camus et al., 2000; Rhinn et al., 1998; Shawlot et al., 1999; Tam and Steiner, 1999). Thus, anterior patterning defects found in nodal hypomorphs may be due to reduced nodal function in the midline mesendoderm as well as in the visceral endoderm. A similar requirement for nodal-related signaling in midline mesendoderm and endoderm formation has been described in zebrafish (Feldman et al., 1998; Gritsman et al., 1999; Sampath et al., 1998). Different levels of nodal signaling have been shown to be necessary for the development of specific cell types in the zebrafish axial midline, with the highest levels required for prechordal plate (Gritsman et al., 2000; Thisse et al., 2000; Thisse and Thisse, 1999). High levels of nodal-related signaling also are required for endoderm development (Schier et al., 1997; Strahle et al., 1997). Our results support a dose-dependent effect for nodal signaling in axial midline and endoderm development in the mouse embryo as well. The least severely affected mutant class, the Type I embryos, lack prechordal plate and the most anterior foregut, and later show forebrain truncations and holoprosencephaly. Type I mutants have a morphologically normal node and, of the three classes of nodal hypomorphs, show the highest *nodal* expression levels in the node. All Type II embryos lack prechordal plate and have a deficiency of notochord in the head, with some also lacking notochord in the trunk. These embryos lack foregut, have a smaller and precociously closed hindgut, and a morphologically abnormal node. There is an accumulation of endoderm or mesendoderm at the level of the node that projects into the hindgut diverticulum, suggesting abnormal migration of the endoderm that does develop. Expression levels in the nodes of Type II embryos varied but were always well below normal. Type III embryos had *nodal*-positive cells in what might represent a disorganized node, and consistently developed a notochord while lacking prechordal plate. Type III mutants completely lack gut endoderm. Our results are consistent with a requirement for high *nodal* levels in the node for correct development of the prechordal plate and foregut, and lower levels required for notochord, node and hindgut formation.

Nodal signaling is required for visceral LR asymmetry

While nodal signaling has been implicated in LR patterning in many vertebrates, it has been difficult to assess in the mouse, owing to the phenotypic severity of the *nodal* null allele. Our analysis of Type I embryos, which lack left LPM *nodal* expression, has allowed us to demonstrate the critical role nodal plays in LR development of the heart, as well as of the cardio-vasculature, lungs and stomach. This function has been thought to be mediated, at least in part, by the transcriptional regulator *Pitx2*, a presumed target of nodal signaling in the left

LPM (Campione et al., 1999; Logan et al., 1998; Ryan et al., 1998). Indeed, our analysis of Type I mutants confirms *Pitx2* as a downstream target gene. There is no LPM expression of *Pitx2* in Type I mutants, and the lungs show a right isomerism phenotype identical to that found in *Pitx2* mutants (Gage et al., 1999; Lin et al., 1999; Lu et al., 1999). This indicates a nodal-to-Pitx2 pathway in the proper development of asymmetry in the lungs, which must involve inhibition of branching normally occurring on the left side. However, targeted mutation of *Pitx2* has no affect on cardiac asymmetry, whereas reduced nodal function does affect the direction of heart looping. Thus, other downstream targets of nodal signaling, still to be identified, are required for ensuring the proper orientation of the developing heart. Another proposed target of nodal signaling is *lefty-2*, which encodes an antagonist of nodal signaling (Bisgrove et al., 1999; Cheng et al., 2000; Meno et al., 1999; Thisse et al., 2000). Indeed, Type I mutants lack *lefty-2* expression in the LPM. Unexpectedly, expression of *lefty-1* also is missing, indicating that it is also a target for nodal. The loss of *lefty-1* may result because the reduced level of nodal activity in the node falls below a critical threshold for activation or maintenance of *lefty-1* expression. It is possible that *nodal* expression in the node does not become asymmetric in Type I mutants. This might be due to the lack of *lefty-1*. Therefore, the LR patterning abnormalities we find in Type I mutants may be due not only to the lack of LPM expression of *nodal*, but also to reduced and symmetric nodal signaling around the node.

In addition to randomized LR cardiac asymmetry, Type I embryos show outflow tract defects. Transpositions of the great vessels were seen in every mutant, regardless of cardiac orientation, and were also found in the small fraction of *nodal*$^{fl1/\Delta}$ embryos that otherwise had no detectable defects. This suggests that the process of conotruncal septation is extremely sensitive to nodal levels. Interventricular septal defects were also found. Thus, it is clear that nodal function in cardiovascular development is more than just to supply cues for sidedness. It also is required for fundamental morphological structuring of the heart and vasculature.

Abdominal LR defects were found in Type I mutants at only a very low frequency. This contrasts with the randomized sidedness of stomachs in *cryptic* mutants (Yan et al., 1999). *Cryptic* mutants do not express nodal in the LPM and are presumed to have a block in nodal signaling around the node, whereas Type I mutants retain some level of nodal activity around the node. Therefore we can speculate that nodal signaling from the node plays some role in stomach handedness. This signaling role may be for the proper development of endoderm that later contributes to stomach development, and thus is only indirectly responsible for stomach laterality. In some *nodal* mutants, the stomach was located dorsal to the lungs, indicating a failure of elongation of the esophagus. These individuals also had underdeveloped lungs, suggesting a connection between esophageal and lung growth. The esophageal growth defect is probably unrelated to the process of stomach rotation, as undescended stomachs were found on either the left or right side of *nodal* mutants. This phenotype has not been described previously and may indicate another target tissue for nodal signaling, or again reflect an endoderm defect stemming from reduced nodal function at an earlier stage.

In summary, the analysis of the *nodal* hypomorphic mutation has permitted the dissection of multiple aspects of nodal function in the developing mouse embryo. Our study shows that nodal signaling, in addition to being essential for mesoderm formation, regulates AP positioning and anterior patterning, midline development, endoderm and gut formation, and LR specification. Further elucidation of nodal function in these early developmental processes will benefit from the application of conditional mutagenic approaches, using stage- and tissue-specific Cre transgenic lines as they become available, in conjunction with floxed *nodal* mice.

We thank Marnie Halpern, Susan Mackem and Shai Izraeli for critical comments on the manuscript.

REFERENCES

Agius, E., Oelgeschlager, M., Wessely, O., Kemp, C. and De Robertis, E. M. (2000). Endodermal Nodal-related signals and mesoderm induction in Xenopus. *Development* **127**, 1173-1183.

Bachiller, D., Klingensmith, J., Kemp, C., Belo, J. A., Anderson, R. M., May, S. R., McMahon, J. A., McMahon, A. P., Harland, R. M., Rossant, J. and De Robertis, E. M. (2000). The organizer factors Chordin and Noggin are required for mouse forebrain development. *Nature* **403**, 658-661.

Beddington, R. S. and Robertson, E. J. (1998). Anterior patterning in mouse. *Trends Genet.* **14**, 277-284.

Beddington, R. S. and Robertson, E. J. (1999). Axis development and early asymmetry in mammals. *Cell* **96**, 195-209.

Belo, J. A., Bouwmeester, T., Leyns, L., Kertesz, N., Gallo, M., Follettie, M. and De Robertis, E. M. (1997). Cerberus-like is a secreted factor with neutralizing activity expressed in the anterior primitive endoderm of the mouse gastrula. *Mech. Dev.* **68**, 45-57.

Biben, C., Stanley, E., Fabri, L., Kotecha, S., Rhinn, M., Drinkwater, C., Lah, M., Wang, C. C., Nash, A., Hilton, D., Ang, S. L., Mohun, T. and Harvey, R. P. (1998). Murine cerberus homologue mCer-1: a candidate anterior patterning molecule. *Dev. Biol.* **194**, 135-151.

Bisgrove, B. W., Essner, J. J. and Yost, H. J. (1999). Regulation of midline development by antagonism of lefty and nodal signaling. *Development* **126**, 3253-3262.

Bouwmeester, T. and Leyns, L. (1997). Vertebrate head induction by anterior primitive endoderm. *BioEssays* **19**, 855-863.

Buchholz, F., Angrand, P. O. and Stewart, A. F. (1996). A simple assay to determine the functionality of Cre or FLP recombination targets in genomic manipulation constructs. *Nucleic Acids Res.* **24**, 3118-3119.

Burdine, R. D. and Schier, A. F. (2000). Conserved and divergent mechanisms in left-right axis formation. *Genes Dev.* **14**, 763-776.

Burgess, R., Cserjesi, P., Ligon, K. L. and Olson, E. N. (1995). Paraxis: a basic helix-loop-helix protein expressed in paraxial mesoderm and developing somites. *Dev. Biol.* **168**, 296-306.

Buzin, C. H., Mann, J. R. and Singer-Sam, J. (1994). Quantitative RT-PCR assays show Xist RNA levels are low in mouse female adult tissue, embryos and embryoid bodies. *Development* **120**, 3529-3536.

Campione, M., Steinbeisser, M., Schweickert, A., Deissler, K., van Bebber, F., Lowe, L. A., Nowotschin, S., Viebahn, C., Haffter, P., Kuehn, M. R. and Blum, M. (1999). The homeobox gene Pitx2: mediator of asymmetric left-right signaling in vertebrate heart and gut looping. *Development* **126**, 1225-1234.

Camus, A., Davidson, B. P., Billiards, S., Khoo, P., Rivera-Perez, J. A., Wakamiya, M., Behringer, R. R. and Tam, P. P. (2000). The morphogenetic role of midline mesendoderm and ectoderm in the development of the forebrain and the midbrain of the mouse embryo. *Development* **127**, 1799-1813.

Capdevila, J., Vogan, K. J., Tabin, C. J. and Izpisua Belmonte, J. C. (2000). Mechanisms of left-right determination in vertebrates. *Cell* **101**, 9-21.

Chen, J. N., van Eeden, F. J., Warren, K. S., Chin, A., Nusslein-Volhard, C., Haffter, P. and Fishman, M. C. (1997). Left-right pattern of cardiac BMP4 may drive asymmetry of the heart in zebrafish. *Development* **124**, 4373-4382.

Cheng, A. M., Thisse, B., Thisse, C. and Wright, C. V. (2000). The lefty-related factor Xatv acts as a feedback inhibitor of Nodal signaling in

mesoderm induction and L-R axis development in Xenopus. *Development* **127**, 1049-1061.
Collignon, J., Varlet, I. and Robertson, E. J. (1996). Relationship between asymmetric nodal expression and the direction of embryonic turning. *Nature* **381**, 155-158.
Conlon, F. L., Barth, K. S. and Robertson, E. J. (1991). A novel retrovirally induced embryonic lethal mutation in the mouse: assessment of the developmental fate of embryonic stem cells homozygous for the 413.d proviral integration. *Development* **111**, 969-981.
Conlon, F. L., Lyons, K. M., Takaesu, N., Barth, K. S., Kispert, A., Herrmann, B. and Robertson, E. J. (1994). A primary requirement for nodal in the formation and maintenance of the primitive streak in the mouse. *Development* **120**, 1919-1928.
Ding, J., Yang, L., Yan, Y. T., Chen, A., Desai, N., Wynshaw-Boris, A. and Shen, M. M. (1998). Cripto is required for correct orientation of the anterior-posterior axis in the mouse embryo. *Nature* **395**, 702-707.
Feldman, B., Gates, M. A., Egan, E. S., Dougan, S. T., Rennebeck, G., Sirotkin, H. I., Schier, A. F. and Talbot, W. S. (1998). Zebrafish organizer development and germ-layer formation require nodal-related signals. *Nature* **395**, 181-185.
Fujinaga, M., Lowe, L. A. and Kuehn, M. R. (2000). α1 adrenergic stimulation perturbs the left-right asymmetric expression pattern of *nodal* during rat embryogenesis. *Teratology* **62**, 317-324.
Gage, P. J., Suh, H. and Camper, S. A. (1999). Dosage requirement of Pitx2 for development of multiple organs. *Development* **126**, 4643-4651.
Gritsman, K., Zhang, J., Cheng, S., Heckscher, E., Talbot, W. S. and Schier, A. F. (1999). The EGF-CFC protein one-eyed pinhead is essential for nodal signaling. *Cell* **97**, 121-132.
Gritsman, K., Talbot, W. S. and Schier, A. F. (2000). Nodal signaling patterns the organizer. *Development* **127**, 921-932.
Hatta, K., Kimmel, C. B., Ho, R. K. and Walker, C. (1991). The cyclops mutation blocks specification of the floor plate of the zebrafish central nervous system. *Nature* **350**, 339-341.
Heisenberg, C. P. and Nusslein-Volhard, C. (1997). The function of silberblick in the positioning of the eye anlage in the zebrafish embryo. *Dev. Biol.* **184**, 85-94.
Hermesz, E., Mackem, S. and Mahon, K. A. (1996). Rpx: a novel anterior-restricted homeobox gene progressively activated in the prechordal plate, anterior neural plate and Rathke's pouch of the mouse embryo. *Development* **122**, 41-52.
Herrmann, B. G. (1991). Expression pattern of the Brachyury gene in whole mount T^{wis}/T^{wis} mutant embryos. *Development* **113**, 913-917.
Heyer, J., Escalante-Alcalde, D., Lia, M., Boettinger, E., Edelmann, W., Stewart, C. L. and Kucherlapati, R. (1999). Postgastrulation Smad2-deficient embryos show defects in embryo turning and anterior morphogenesis. *Proc. Natl. Acad. Sci. USA* **96**, 12595-12600.
Heymer, J., Kuehn, M. and Ruther, U. (1997). The expression pattern of nodal and lefty in the mouse mutant Ft suggests a function in the establishment of handedness. *Mech. Dev.* **66**, 5-11.
Iannaccone, P. M., Zhou, X., Khokha, M., Boucher, D. and Kuehn, M. R. (1992). Insertional mutation of a gene involved in growth regulation of the early mouse embryo. *Dev. Dyn.* **194**, 198-208.
Izraeli, S., Lowe, L. A., Bertness, V. L., Good, D. J., Dorward, D. W., Kirsch, I. R. and Kuehn, M. R. (1999). The SIL gene is required for mouse embryonic axial development and left- right specification. *Nature* **399**, 691-694.
Jones, C. M., Kuehn, M. R., Hogan, B. L. M., Smith, J. C. and Wright, C. V. E. (1995). Nodal-related signals induce axial mesoderm and dorsalize mesoderm during gastrulation. *Development* **121**, 3651-3662.
Joseph, E. M. and Melton, D. A. (1997). Xnr4: a Xenopus nodal-related gene expressed in the Spemann organizer. *Dev. Biol.* **184**, 367-372.
Kumar, A., Novoselov, V., Celeste, A. J., Wolfman, N. M., ten Dijke, P. and Kuehn, M. R. (2001). Nodal signaling uses activin and transforming growth factor-beta receptor-regulated smads. *J. Biol. Chem.* **276**, 656-661.
Lakso, M., Pichel, J. G., Gorman, J. R., Sauer, B., Okamoto, Y., Lee, E., Alt, F. W. and Westphal, H. (1996). Efficient in vivo manipulation of mouse genomic sequences at the zygote stage. *Proc. Natl. Acad. Sci. USA* **93**, 5860-5865.
Levin, M., Johnson, R. L., Stern, C. D., Kuehn, M. and Tabin, C. (1995). A molecular pathway determining left-right asymmetry in chick embryogenesis. *Cell* **82**, 803-814.
Levin, M., Pagan, S., Roberts, D. J., Cooke, J., Kuehn, M. R. and Tabin, C. J. (1997). Left/right patterning signals and the independent regulation of different aspects of situs in the chick embryo. *Dev. Biol.* **189**, 57-67.
Lin, C. R., Kioussi, C., O'Connell, S., Briata, P., Szeto, D., Liu, F., Izpisua-Belmonte, J. C. and Rosenfeld, M. G. (1999). Pitx2 regulates lung asymmetry, cardiac positioning and pituitary and tooth morphogenesis. *Nature* **401**, 279-282.
Logan, M., Pagan-Westphal, S. M., Smith, D. M., Paganessi, L. and Tabin, C. J. (1998). The transcription factor Pitx2 mediates situs-specific morphogenesis in response to left-right asymmetric signals. *Cell* **94**, 307-317.
Lowe, L. A., Supp, D. M., Sampath, K., Yokoyama, T., Wright, C. V., Potter, S. S., Overbeek, P. and Kuehn, M. R. (1996). Conserved left-right asymmetry of nodal expression and alterations in murine situs inversus. *Nature* **381**, 158-161.
Lowe, L. A. and Kuehn, M. R. (2000). Whole mount in situ hybridization to study gene expression during mouse development. In *Developmental Biology Protocols*. Vol. III (ed. R. S. Tuan and C. W. Lo), pp. 125-137. Totowa, NJ: Humana.
Lu, M. F., Pressman, C., Dyer, R., Johnson, R. L. and Martin, J. F. (1999). Function of Rieger syndrome gene in left-right asymmetry and craniofacial development. *Nature* **401**, 276-278.
Lustig, K. D., Kroll, K., Sun, E., Ramos, R., Elmendorf, H. and Kirschner, M. W. (1996). A Xenopus nodal-related gene that acts in synergy with noggin to induce complete secondary axis and notochord formation. *Development* **122**, 3275-3282.
Marth, J. D. (1996). Recent advances in gene mutagenesis by site-directed recombination. *J. Clin. Invest.* **97**, 1999-2002.
Melloy, P. G., Ewart, J. L., Cohen, M. F., Desmond, M. E., Kuehn, M. R. and Lo, C. W. (1998). No turning, a mouse mutation causing left-right and axial patterning defects. *Dev. Biol.* **193**, 77-89.
Meno, C., Gritsman, K., Ohishi, S., Ohfuji, Y., Heckscher, E., Mochida, K., Shimono, A., Kondoh, H., Talbot, W. S., Robertson, E. J., Schier, A. F. and Hamada, H. (1999). Mouse Lefty2 and zebrafish antivin are feedback inhibitors of nodal signaling during vertebrate gastrulation. *Mol. Cell* **4**, 287-298.
Mountford, P., Zevnik, B., Duwel, A., Nichols, J., Li, M., Dani, C., Robertson, M., Chambers, I. and Smith, A. (1994). Dicistronic targeting constructs: reporters and modifiers of mammalian gene expression. *Proc. Natl. Acad. Sci. USA* **91**, 4303-4307.
Nomura, M. and Li, E. (1998). Smad2 role in mesoderm formation, left-right patterning and craniofacial development. *Nature* **393**, 786-790.
Oh, S. P. and Li, E. (1997). The signaling pathway mediated by the type IIB activin receptor controls axial patterning and lateral asymmetry in the mouse. *Genes Dev.* **11**, 1812-1826.
Osada, S. I. and Wright, C. V. (1999). Xenopus nodal-related signaling is essential for mesendodermal patterning during early embryogenesis. *Development* **126**, 3229-3240.
Pfendler, K. C., Yoon, J., Taborn, G. U., Kuehn, M. R. and Iannaccone, P. M. (2000). Nodal and bone morphogenetic protein 5 interact in murine mesoderm formation and implantation. *Genesis* **28**, 1-14.
Rebagliati, M. R., Toyama, R., Fricke, C., Haffter, P. and Dawid, I. B. (1998a). Zebrafish nodal-related genes are implicated in axial patterning and establishing left-right asymmetry. *Dev. Biol.* **199**, 261-272.
Rebagliati, M. R., Toyama, R., Haffter, P. and Dawid, I. B. (1998b). cyclops encodes a nodal-related factor involved in midline signaling. *Proc. Natl. Acad. Sci. USA* **95**, 9932-9937.
Rhinn, M., Dierich, A., Shawlot, W., Behringer, R. R., Le Meur, M. and Ang, S. L. (1998). Sequential roles for Otx2 in visceral endoderm and neuroectoderm for forebrain and midbrain induction and specification. *Development* **125**, 845-856.
Ryan, A. K., Blumberg, B., Rodriguez-Esteban, C., Yonei-Tamura, S., Tamura, K., Tsukui, T., de la Pena, J., Sabbagh, W., Greenwald, J., Choe, S. et al. (1998). Pitx2 determines left-right asymmetry of internal organs in vertebrates. *Nature* **394**, 545-551.
Saijoh, Y., Adachi, H., Sakuma, R., Yeo, C. Y., Yashiro, K., Watanabe, M., Hashiguchi, H., Mochida, K., Ohishi, S., Kawabata, M. et al. (2000). Left-right asymmetric expression of lefty2 and nodal is induced by a signaling pathway that includes the transcription factor FAST2. *Mol. Cell* **5**, 35-47.
Sampath, K., Cheng, A. M., Frisch, A. and Wright, C. V. (1997). Functional differences among Xenopus nodal-related genes in left-right axis determination. *Development* **124**, 3293-3302.
Sampath, K., Rubinstein, A. L., Cheng, A. M., Liang, J. O., Fekany, K., Solnica-Krezel, L., Korzh, V., Halpern, M. E. and Wright, C. V. (1998). Induction of the zebrafish ventral brain and floorplate requires cyclops/nodal signalling. *Nature* **395**, 185-189.

Schier, A. F., Neuhauss, S. C., Helde, K. A., Talbot, W. S. and Driever, W. (1997). The one-eyed pinhead gene functions in mesoderm and endoderm formation in zebrafish and interacts with no tail. *Development* **124**, 327-342.

Schier, A. F. and Shen, M. M. (2000). Nodal signalling in vertebrate development. *Nature* **403**, 385-389.

Shawlot, W., Deng, J. M. and Behringer, R. R. (1998). Expression of the mouse cerberus-related gene, Cerr1, suggests a role in anterior neural induction and somitogenesis. *Proc. Natl. Acad. Sci. USA* **95**, 6198-6203.

Shawlot, W., Wakamiya, M., Kwan, K. M., Kania, A., Jessell, T. M. and Behringer, R. R. (1999). Lim1 is required in both primitive streak-derived tissues and visceral endoderm for head formation in the mouse. *Development* **126**, 4925-4932.

Simeone, A., Acampora, D., Mallamaci, A., Stornaiuolo, A., D'Apice, M. R., Nigro, V. and Boncinelli, E. (1993). A vertebrate gene related to orthodenticle contains a homeodomain of the bicoid class and demarcates anterior neuroectoderm in the gastrulating mouse embryo. *EMBO J.* **12**, 2735-2747.

Smith, W. C., McKendry, R., Ribisi, S., Jr. and Harland, R. M. (1995). A nodal-related gene defines a physical and functional domain within the Spemann organizer. *Cell* **82**, 37-46.

Song, J., Oh, S. P., Schrewe, H., Nomura, M., Lei, H., Okano, M., Gridley, T. and Li, E. (1999). The type II activin receptors are essential for egg cylinder growth, gastrulation, and rostral head development in mice. *Dev. Biol.* **213**, 157-169.

Strahle, U., Jesuthasan, S., Blader, P., Garcia-Villalba, P., Hatta, K. and Ingham, P. W. (1997). one-eyed pinhead is required for development of the ventral midline of the zebrafish (Danio rerio) neural tube. *Genes Funct.* **1**, 131-148.

Tam, P. P. and Steiner, K. A. (1999). Anterior patterning by synergistic activity of the early gastrula organizer and the anterior germ layer tissues of the mouse embryo. *Development* **126**, 5171-5179.

Thisse, B., Wright, C. V. and Thisse, C. (2000). Activin- and Nodal-related factors control antero-posterior patterning of the zebrafish embryo. *Nature* **403**, 425-428.

Thisse, C. and Thisse, B. (1999). Antivin, a novel and divergent member of the TGFbeta superfamily, negatively regulates mesoderm induction. *Development* **126**, 229-240.

Thomas, P. Q., Brown, A. and Beddington, R. S. (1998). Hex: a homeobox gene revealing peri-implantation asymmetry in the mouse embryo and an early transient marker of endothelial cell precursors. *Development* **125**, 85-94.

Toyama, R., O'Connell, M. L., Wright, C. V., Kuehn, M. R. and Dawid, I. B. (1995). Nodal induces ectopic goosecoid and lim1 expression and axis duplication in zebrafish. *Development* **121**, 383-391.

Tremblay, K. D., Hoodless, P. A., Bikoff, E. K. and Robertson, E. J. (2000). Formation of the definitive endoderm in mouse is a Smad2-dependent process. *Development* **127**, 3079-3090.

Varlet, I., Collignon, J. and Robertson, E. J. (1997). nodal expression in the primitive endoderm is required for specification of the anterior axis during mouse gastrulation. *Development* **124**, 1033-1044.

Yan, Y. T., Gritsman, K., Ding, J., Burdine, R. D., Corrales, J. D., Price, S. M., Talbot, W. S., Schier, A. F. and Shen, M. M. (1999). Conserved requirement for EGF-CFC genes in vertebrate left-right axis formation. *Genes Dev.* **13**, 2527-2537.

Zhou, X., Sasaki, H., Lowe, L., Hogan, B. L. and Kuehn, M. R. (1993). Nodal is a novel TGF-beta-like gene expressed in the mouse node during gastrulation. *Nature* **361**, 543-547.